Optimal Linear Quadratic Regulator Design of Interconnected Systems with VSP based HVDC Links for Inertia Emulation

Elyas Rakhshani [(1)], Iman Mohammad Hosseini Naveh[(2)], Hasan Mehrjerdi[(3)], José Rueda Torres[(1)], and Peter Palensky[(1)]

[(1)] Department of Electrical Sustainable Energy, Delft University of Technology, Netherlands
[(2)] Department of Electrical Engineering, Gonabad Branch, Islamic Azad University, Gonabad, Iran
[(3)] Electrical Engineering Department, Qatar University, Doha, Qatar

***Abstract*— This paper proposes a new application for an optimal linear regulator for mitigation of frequency performance of an interconnected AC/DC system with (Virtual Synchronous Power) VSP based HVDC capabilities. The action of VSP, which is added into the HVDC control system, is to provide virtual inertia for the low-inertia system during a contingency. The proposed optimal regulator is designed to stabilize such ac/dc interconnected system while minimizing the associated cost function. For each of the presented controller, a different objective function is defined. This objective function is needed to tune the matrix gains and to process the optimum controller design. Simulations results demonstrate how the proposed regulator can significantly improve the reduction of frequency deviations and the damping of the interarea oscillations excited during a fault. This improvement is more obvious especially when a VSP-based virtual inertia emulation is activated in the system.**

Keywords*— Fast frequency response, Frequency control, Virtual inertia, LQR controller.

I. INTRODUCTION

Frequency control considering different methods for enhancing its dynamic performance is very important especially in modern power system with low-inertia [1]-[5]. Systems with low inertia are the result of the phase-out of the conventional power plants, with a synchronous generator, due to increasing the share of power electronic-based components like HVDC links, solar photovoltaic systems and wind power plants [6]-[11]. Frequency dynamics are much faster in power systems with low inertia, and it makes the frequency control and power system operation more difficult. Thus, considering the intermitted behavior in this kind of system, developing an additional supplementary control loop for facilitating fast frequency response capabilities of power electronic-based generation units are very important.

New ideas such as synthetic inertia emulation (IE) [12] and virtual synchronous generator (VSG) are among the main research in this topic [13]. Usually, virtual inertia can be emulated using an advanced controller for high power converters. It may need a short term source of energy for enabling an effective virtual inertia emulation. To date, many authors have tried to propose different approaches for embedding the behavior of synchronous machines in control system used by power converters [14]–[17]. According to these reports, different methodologies are used for modifying the power reference of the electronic converters to provide synthetic inertia to the system.

Application of derivative control for emulating virtual inertia in HVDC interconnected power systems is one of the common approaches at the system level [18]–[20]. In most of the derivative and droop based approaches, the input signal for inertia emulation controller is the frequency error. Therefore, the confident measurement of frequency in those methods is very important, and the application of different techniques for frequency measurements like (Phase-Locked Loop) PLL may have some limitations. Thus, an alternative controller for an automatic generation control application (AGC), which is based on Virtual Synchronous Power (VSP) strategy is proposed in [21]. In this approach, the input signal of the inertia emulation controller is the power deviation instead of frequency in derivative-based methods. The main control loop in the VSP approach has a second-order behavior, which makes it possible to influence the system with both damping and inertia emulation at the same time.

In this paper, the main objective for modeling and controlling of an interconnected AC/DC system with VSP capabilities are: Applying a new advanced control approach for high-level application, defining a suitable model with a global feedback law and determining the required energy during inertia emulation after the occurrence of the fault. Therefore, to tackle these issues, the design and control of the system with an optimal linear quadratic regulator (LQR) for an AC/DC system facilitated by VSP capabilities is proposed. In this method, the optimal control law was determined by minimizing a suitable performance index under the state feedback conditions. So the matrix equations are solved optimally to find the best feedback gains with an acceptable dynamics response for the system's states.

The proposed control approach is tested on a two-area power system under different conditions. The obtained results from the designed optimal LQR controller for the system with VSP is compared with other classical AC/DC models. Simulation results are verified the excellent performance of the proposed control approach during dynamic and steady-state operational conditions.

The rest of the paper is structured as the following. In Section II, the mathematical representation for the studied models, a two-area interconnected model, the model with DC link and the model considering VSP capabilities, are presented. Later, in Section III, the control structures and the designed controller is explained. While the simulation results and conclusions are presented by Sections IV and V, respectively.

II. Mathematical Model of Interconnected Power System

A typical system for presenting a general model of interconnected systems is a modified Kundur model as an interconnected model with two areas which is shown in Figure 1. It has two GENCOs (Generation Company) and one DISCOs (Distribution Company) as a load in each area. DISCOs can be considered as load demands.

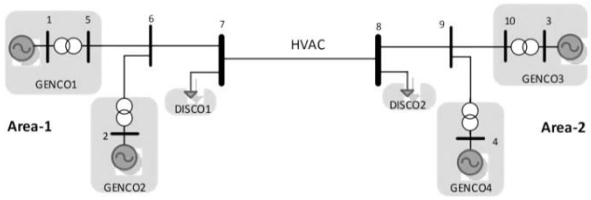

Fig. 1. A two-area system with an AC connection.

As explained in [3] and [6], this model will have nine state consists of frequency in each area (two areas), output power for each unit (four units in total), area control error signal (ACE) for each area and power deviations in the AC link. Thus, the closed-loop system for LFC with two areas inter-connected system can be presented in the form of state space as follows:

$$\Delta\dot{X}_{LFC} = A_{9\times9}\Delta X_{LFC} + B_{9\times2}\Delta U_{LFC} \quad (1)$$

$$\Delta U_{LFC} = [\Delta P_{d1} \;\; \Delta P_{d2}]^T \quad (2)$$

$$\Delta X_{LFC} = [\Delta\omega_1 \;\; \Delta\omega_2 \;\; \Delta P_{m1} \;\; \Delta P_{m2} \;\; \Delta P_{m3} \;\; \Delta P_{m4} \;\; \int ACE_1 \;\; \int ACE_2 \;\; \Delta P_{tieAC,12} \;\;]^T \quad (3)$$

The general structure of the test model with two areas and a parallel AC/DC link is presented in Figure 2. In this case, one more state from the DC link will be added to the state-space model of the interconnected system. More details about this modelling can be found in [6].

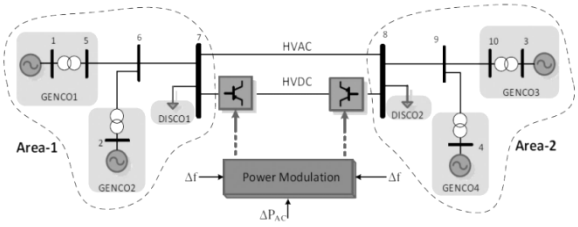

Fig. 2. A schematic diagram of a two-area AGC model with a parallel AC/HVDC link

The closed-loop system of this two area model with a DC link can be presented in the form of a state space:

$$\Delta\dot{X}_{HVDC} = A_{10\times10}\Delta X_{HVDC} + B_{10\times2}\Delta U_{HVDC} \quad (4)$$

$$\Delta U_{HVDC} = [\Delta P_{d1} \;\; \Delta P_{d2}]^T \quad (5)$$

$$\Delta X_{LFC} = [\Delta\omega_1 \;\; \Delta\omega_2 \;\; \Delta P_{m1} \;\; \Delta P_{m2} \;\; \Delta P_{m3} \;\; \Delta P_{m4} \;\; \Delta P_{ref1} \;\; \Delta P_{ref2} \;\; \Delta P_{tieAC,12} \;\; \Delta P_{DC} \;\;]^T \quad (6)$$

where $\Delta\omega_i$ (i = 1,2) is the frequency deviation of each area in p.u., ΔP_{mk} (k = 1,2,3,4) is the output power of each generation unit, ΔP_{refi} is the set point for each generator coming from area control error, ΔP_{DC} is the DC power deviation and $\Delta P_{tieAC,12}$ is the deviation in the AC transmitted power. Furthermore, as shown in Figure 3, it is assumed that the AC model in Figure 1 is modified by adding a parallel AC/HVDC link between area *i* and Area *k*, where both converter stations of the HVDC link are facilitated by VSP functionalities.

Therefore, in a two-area AC/DC interconnected power system, which will have two synchronous controllers, four new states variables of synchronous controllers will be added to the system [21]. The overall system will have thirteen state variables as it is written as follows:

$$\Delta\dot{X}_{VSPHVDC} = A_{13\times13}\Delta X_{VSPHVDC} + B_{13\times2}\Delta U_{VSPHVDC} \quad (7)$$

$$\Delta U_{VSPHVDC} = [\Delta P_{L1} \;\; \Delta P_{L2}]^T \quad (8)$$

$$\Delta X_{LFC} = [\Delta\omega_1 \;\; \Delta\omega_2 \;\; \Delta P_{m1} \;\; \Delta P_{m2} \;\; \Delta P_{m3} \;\; \Delta P_{m4} \;\; \Delta ACE_1 \;\; \Delta ACE_2 \;\; \Delta x_{p,vsp1} \; \Delta x_{f,vsp1} \;\; \Delta x_{p,vsp2} \;\; \Delta x_{f,vsp2} \;\;]^T \quad (9)$$

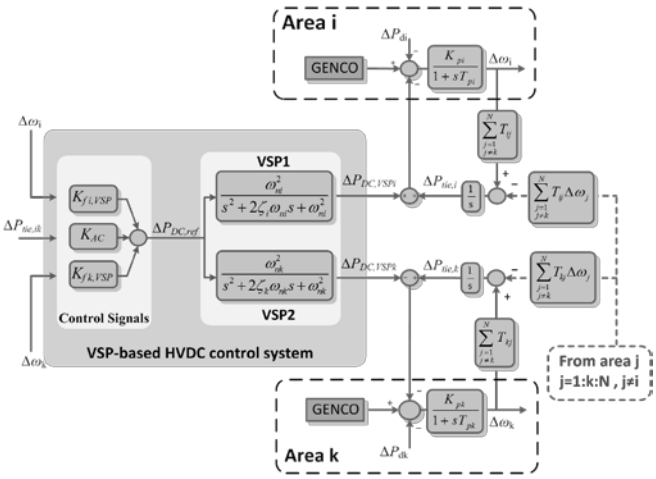

Fig. 3. The basic frame of AGC in multi-area systems with a VSP based AC/DC transmission.

While $\Delta x_{p,vsp}$ represents the emulated power and $\Delta x_{f,vsp}$ is the derivative term of this power for each VSP. Therefore, the unit of $\Delta x_{p,vsp}$ is in terms of Megawatt (MW). More details about the state matrix and all the state space equations can be found in [21].

III. Optimal Control Scenarios

A. Linear Quadratic Regulator Design for State Variables

This section briefly introduces the optimal control theory for the proposed LQR controller. The main goal of a linear-quadratic optimal controller is the stabilization and dynamic improvement of a system, by minimizing the magnitude of it's associated cost function. So considering the above explanations, the performance index (J) can be usually defined by equation (16) [22]–[24]. This cost function is needed to tune the matrix gain Q and R during the optimization algorithm.

$$J = \int_0^{+\infty} \left(\Delta X_{Sys}{}^T(t) Q \Delta X_{Sys}(t) + \Delta U_{Sys}{}^T(t) R \Delta U_{Sys}(t) \right) dt \quad (10)$$

With the matrix Q being symmetric, semi-definite and positive, and the matrix R can be a positive, symmetric, and definite matrix. In this equation, the first term will be optimized when it is equal to zero. Therefore the first term in the LQR optimization method is called zero – tracking. Also, the second term is referred to as a control effort. On the other hand, the LQR controller is a solution to the optimal control problem where full state feedback is assumed, and the

disturbance input is considered to be zero. The control signal which minimizes the above performance index is given by the feedback control law in terms of system states:

$$\Delta U_{Sys}(t) = -K\Delta X_{Sys}(t) \tag{11}$$

$$K = R^{-1}{B_{Sys}}^{T}P \tag{12}$$

where P is the solution of the Riccati equation:

$${A_{Sys}}^{T}P + PA_{Sys} - PB_{Sys}R^{-1}{B_{Sys}}^{T}P + Q = 0 \tag{13}$$

B. Linear Quadratic Regulator Design for Output Variables

The other linear-quadratic optimal controller which is going to be used will try to stabilize the system performance by minimization of its cost function respect to the output variables. So we can rewrite the cost function by this equation:

$$J = \int_0^{+\infty}\left({\Delta Y_{Sys}}^{T}(t)Q_Y\Delta Y_{Sys}(t) + {\Delta U_{Sys}}^{T}(t)R\,\Delta U_{Sys}(t)\right)dt \tag{14}$$

where Q_Y and R are matrices with the same definitions in the previous scenario. In this equation, the first term will be optimized when outputs are equal to zero. Therefore, the first term in the LQRY optimization method is called output variables zero – tracking.

C. Linear Quadratic Regulator Design with Prescribed Degree of Stability

In this part, a controller with a prescribed degree of stability with focusing on damping of all inter-area oscillation is proposed. This can be done by shifting the eigenvalues of the system to the left-hand side of the S plan. In order to have a better insight about the performance of this controller, the optimal full state feedback control is designed and its results are compared with extended optimal control, called the prescribed degree of stability, as the proposed method.

By using the prescribed degree of stability method, the linear optimal controller can be designed to obtain a special degree of stability in the optimal closed-loop system. In the other hand, we can design a new controller that it can transfer all of the poles of the closed-loop system to the left-hand-side of α (a real value) in the *S* plane [25]-[26]. Thus, in a linear system, the following performance index can be used for the implementation of the control with a prescribed degree of stability:

$$J = \int_0^{+\infty} e^{2\alpha t}\left({\Delta Y_{Sys}}^{T}(t)Q_Y\Delta Y_{Sys}(t) + {\Delta U_{Sys}}^{T}(t)R\,\Delta U_{Sys}(t)\right)dt \tag{15}$$

The control signal which can minimize the performance index in (15), is presented by the feedback control law in terms of system states:

$$\Delta U_{Sys}(t) = -K_\alpha\Delta X_{Sys}(t) \tag{16}$$

$$K_\alpha = R^{-1}{B_{Sys}}^{T}P_\alpha \tag{17}$$

where P_α is the solution for the Riccati equation:

$$\left(A_{Sys} + \alpha I_n\right)^{T}P_\alpha + P\left(A_{Sys} + \alpha I_n\right) - P_\alpha B_{Sys}R^{-1}{B_{Sys}}^{T}P_\alpha + Q = 0 \tag{18}$$

In order to be asymptotically stable for A_α, we can write:

$$\lambda_i(A_\alpha) = \lambda_i\left(A_{Sys} + \alpha I_n - B_{Sys}K_\alpha\right) = \lambda_i\left(A_{Sys} - B_{Sys}K_\alpha\right) + \alpha \tag{19}$$

where $\lambda_i(A_\alpha)$ is eigenvalues of A_α for i=1,2,…n. Because of Real $(\lambda_i(A_\alpha)) < 0$, we can write:

$$Real\left(\lambda_i(A_\alpha)\right) = Real\left(\lambda_i\left(A_{Sys} - B_{Sys}K_\alpha\right)\right) + \alpha < 0 \tag{20}$$

Therefore we have:

$$Real\left(\lambda_i\left(A_{Sys} - B_{Sys}K_\alpha\right)\right) < -\alpha \tag{21}$$

In fact, by considering the optimal control with a prescribed degree of stability control, all of the eigenvalues of the system (A_{Sys} - $B_{Sys}K_\alpha$) will be located on the left-hand side of $-\alpha$ in *S* plane.

IV. Simulation Results

In this section, in order to show the performance of the proposed controller, especially compared to other classical controllers, different simulations are performed for the two area interconnected systems explained in Section II. The simulations are done using the Matlab platform. As shown in Figure 4, step changes inputs as load demand for all mathematical models are based on the following equation:

$$Control\ Input(t) = \begin{cases} 0.03 & 2 \le t < 30 \\ 0.015 & t \ge 30 \\ 0 & otherwise \end{cases} \tag{22}$$

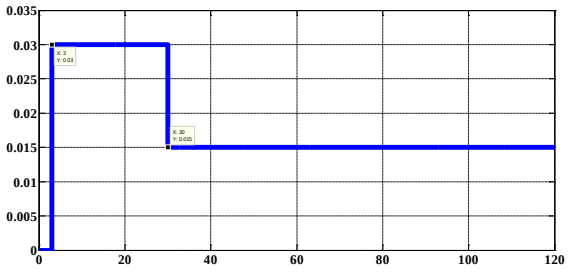

Fig. 4. Control input signal as the step load changes in all simulations.

1. Simulation Results for the First Scenario

By attention to the mathematical model systems presented in Section II, part A, the results of LQR controller for LFC, HVDC, and VSP based HVDC models are presented in Figures 5 and 6. The constant matrixes used to generate its performance index, equation (10), will be selected as follows:

$$LFC\ System: \begin{cases} Q = 1800 \times eye\left(size(A_{LFC})\right) \\ R = 55080 \times eye\left(size(B_{LFC})\right) \end{cases} \tag{23}$$

$$HVDC\ System: \begin{cases} Q = 1800 \times eye\left(size(A_{HVDC})\right) \\ R = 66080 \times eye\left(size(B_{HVDC})\right) \end{cases} \tag{24}$$

$$VSP, HVDC\ System: \begin{cases} Q = 1500 \times eye\left(size(A_{VSPHVDC})\right) \\ R = 55080 \times eye\left(size(B_{VSPHVDC})\right) \end{cases} \quad (25)$$

As shown in Figs. 5 and 6, after the implementation of LQR control, the model with VSP shows superior performance compared to other models.

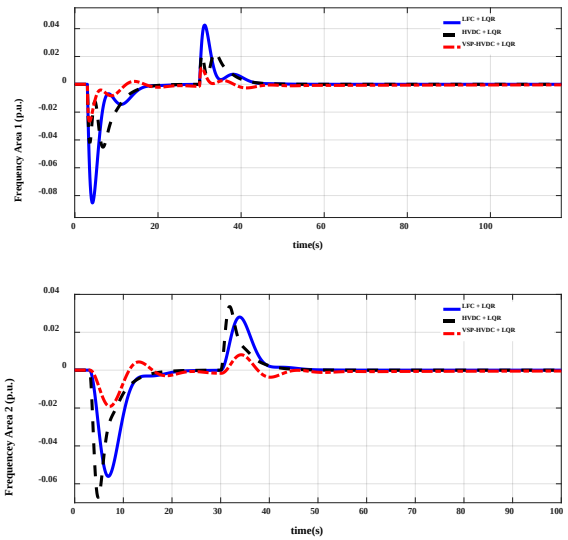

Fig.5. Frequency (pu): comprehensive analysis between mathematical models (LFC, HVDC, VSP-HVDC) in the first scenario, (a) ω_1, (b) ω_2 .

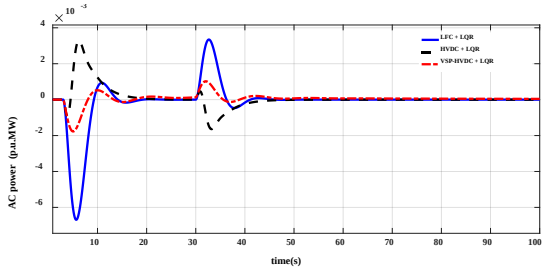

Fig. 6. AC power deviation (pu): comprehensive analysis between mathematical models (LFC, HVDC, VSP-HVDC) in the first scenario.

2. Simulation Results for the Second Scenario

In this section, the performance of the designed LQR controller with the output zero – tracking (as explained in Section II-B) will be evaluated for different models. The test models are the ones presented in Section II for classical LFC in the AC system, HVDC system and the model with VSP based HVDC systems. Thus, the constant matrices used to generate its performance index, equation (14), will be selected as follows:

$$LFC\ System: \quad Q_Y = 150.85 \times eye\left(size(C_{LFC})\right) \quad (26)$$

$$HVDC\ System: \quad Q_Y = 185 \times eye\left(size(C_{HVDC})\right) \quad (27)$$

$$VSP, HVDC\ System: \quad Q_Y = 185 \times eye\left(size(C_{VSPHVDC})\right) \quad (28)$$

As explained in Section III-B, in this controller the cost function is selected according to the output variables. Therefore, as shown in equations (26)-(28), the constant matrices are selected based on the size of output matrix *C* for different models.

The performance of this controller for different models is shown in Figures 7 and 8. Obtained results show the successful implementation of the designed optimal controller for different models, while the model with VSP based HVDC capabilities shows better more improvements in damping of oscillations during faults.

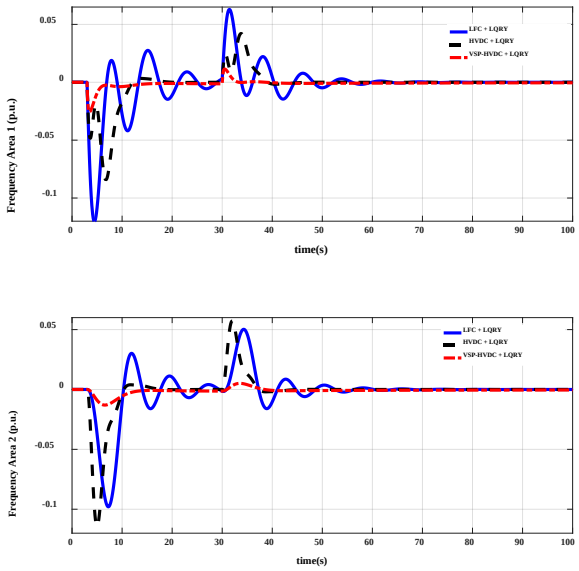

Fig. 7. Frequency in both areas: comprehensive analysis between mathematical models (LFC, HVDC, VSP-HVDC) for the second scenario.

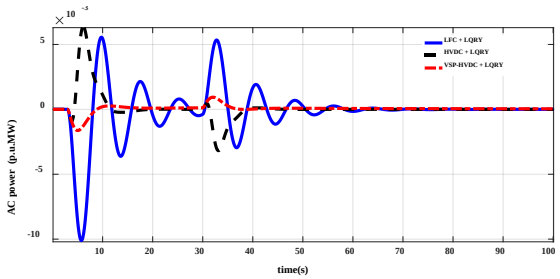

Fig. 8. Comprehensive analysis between mathematical models (LFC, HVDC, VSP-HVDC) in the second scenario for variables: (a) ω_1, (b) ω_2 and (c) AC power deviation.

3. Simulation Results for the Third Scenario

In this section, the application of the controller with a prescribed degree of stability for the two-area interconnected system with VSP based HVDC system is presented. In this simulation, by attention to the linear-quadratic optimal control model based on the prescribed degree of stability, the constant α is around 1.0785. The results are compared with the classical LFC model and the one with normal HVDC link. The dynamics of power flow in the AC line and the response of frequency in both areas are shown in Figures 9 and 10, respectively.

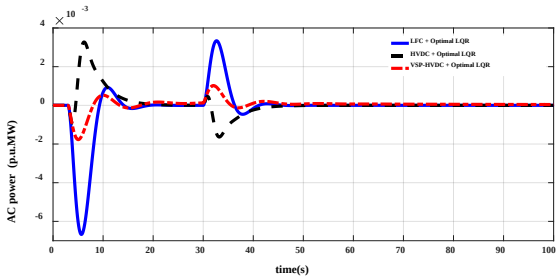

Fig. 9. AC power deviation: comparison between mathematical models (LFC, HVDC, VSP-HVDC) in the third scenario.

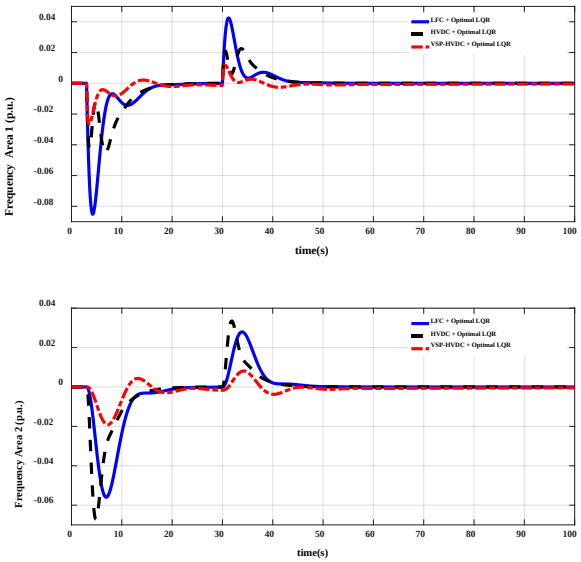

Fig. 10. Frequency deviations: comparisons between mathematical models (LFC, HVDC, VSP-HVDC) in the third scenario for variables: (a) ω_1 ,(b) ω_2.

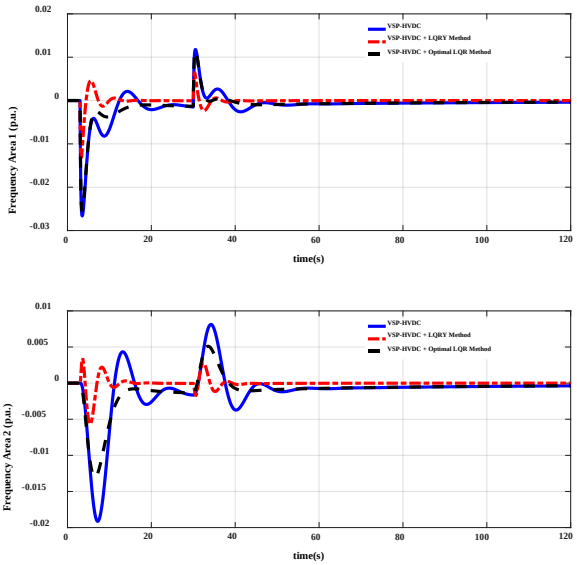

Fig. 11. Comprehensive analysis between linear quadratic regulators in two-area with VSP based HVDC model for variables: (a) ω_1 and (b) ω_2.

4. *Simulation Results Based on Comparison Between Scenarios*

In this section, the performances of different controllers presented in the previous section are compared. According to the obtained results in Section IV-1 to IV-3, it becomes clear that in all control strategies the performance of the model with VSP based HVDC system is much better. This can be evident considering the location of dominant eigenvalues for different models:

a. Dominant eigenvalues for the classical LFC Model, in the state feedback simulation:

$$eig_{LFC} = \begin{bmatrix} -0.1425 - 0.8256i & -0.1425 + 0.8256i & -0.4573 - 0.3995i \dots \\ -0.4573 + 0.3995i & -0.8173 + 0.0000i & -1.9421 + 0.0000i \dots \\ -2.2223 + 0.0000i & -2.8022 + 0.0000i & -2.7466 + 0.0000i \end{bmatrix} \quad (29)$$

b. Dominant eigenvalues for the model with HVDC link in the state feedback simulation:

$$eig_{HVDC} = \begin{bmatrix} -24.7198 + 0.0000i & -0.5108 - 1.7160i & -0.5108 + 1.7160i \dots \\ -0.3551 - 0.4385i & -0.3551 + 0.4385i & -0.9270 + 0.0000i \dots \\ -2.0013 - 0.1809i & -2.0013 + 0.1809i & -2.7736 + 0.0000i \dots \\ & -2.7184 + 0.0000i & \end{bmatrix} \quad (30)$$

c. Dominant eigenvalues for the model with VSP based HVDC system in the state feedback simulation:

$$eig_{VSPHVDC} = \begin{bmatrix} -30.1645 + 0.0000i & -20.2944 + 0.0000i & -2.8407 + 0.0000i \dots \\ -1.9028 - 0.9753i & -1.9028 + 0.9753i & -0.3803 - 1.1152i \dots \\ -0.3803 + 1.1152i & -1.2052 + 0.0000i & -0.0938 + 0.0000i \dots \\ -0.0174 + 0.0000i & -4.1941 + 0.0000i & -5.3342 + 0.0000i \dots \\ & -5.2237 + 0.0000i & \end{bmatrix} \quad (31)$$

Therefore, as shown in Figure 11, a generic comparison for different optimal controller for the two-area model with VSP based HVDC system is performed. The response of the frequency in both areas are presented in Figure 11. It is clear that in all control scenarios, the controller with a prescribed degree of stability (called optimal linear quadratic regulator method) has a better effect than others.

V. Conclusion

The concept of virtual inertia emulation in AC/DC interconnected system with different advanced controller for higher-level applications for frequency control issue has been discussed and presented in this paper. According to the literature review in this paper, proposition of proper advanced controller for system components are as important as the implementation of new concepts like virtual inertia emulation. In the future modern power system, advanced supervisory control, with proper coordination between generation units will be critical.

Different analysis for different optimal regulators for an interconnected LFC system with VSP based HVDC capabilities has been discussed. It shows how different advanced control can be implemented by defining a suitable model with a global feedback law. The studied controllers are the linear quadratic regulator for all states and outputs with zero tracking target and also an optimal regulator based on the prescribed degree of stability.

By attention to the simulation results presented in Sections 1, 2 and 3, it can be observed that the proposed controller for the system with VSP based HVDC system, as a new model, gives better results and therefore better damping and satisfactory accuracy versus LFC and HVDC model. Thanks to the proposed controller with a prescribed degree of stability, the modes of the system are shifted to a better location which makes it possible to control the states with minimum oscillations and with less sensitivity to the plant parameter variations. The proposed control approach can be implied to different systems with any type of complexity.

Acknowledgment

This research was carried out as part of the MIGRATE project. This project has received funding from the European Union's Horizon 2020 research and innovation program under grant agreement No 691800. This reflects only the authors' views and the European Commission is not responsible for any use that may be made of the information it contains.

REFERENCES

[1] P. Kundur et al., "Definition and Classification of Power System Stability," *IEEE Trans. Power Syst.*, Vol. 19, No. 3, pp. 1387–1401, 2004.

[2] P. Tielens and D. Van Hertem, "The relevance of inertia in power systems," *Renew. Sustain. Energy Rev.*, vol. 55, pp. 999–1009, 2016.

[3] E. Rakhshani, J. Sadeh, "Practical Viewpoints on Load Frequency Control Problem in a Deregulated Power System", *Energy conversion and management*, Vol. 51. Issue 6. pp. 1148-1156. June 2010.

[4] Hasan Mehrjerdi, Elyas Rakhshani, "Vehicle-to-grid technology for cost reduction and uncertainty management integrated with solar power," *Journal of Cleaner Production*, Elsevier, Vol .229, pp. 463-469, 2019.

[5] Hasan Mehrjerdi, Elyas Rakhshani, "Optimal operation of hybrid electrical and thermal energy storage systems under uncertain loading condition," *Applied Thermal Engineering*, Elsevier, Vol. 160, 2019.

[6] E. Rakhshani, P. R. Cortes, "Inertia Emulation in AC/DC Power Systems Using Derivative Technique Considering Frequency Measurement Effects", *IEEE Transactions on Power Systems*, Volume: 32, Issue: 5, 2017.

[7] R. Eriksson, N. Modig, and K. Elkington, "Synthetic inertia versus fast frequency response : a definition," *IET Renew. Power Gener.*, Vol. 12, No. 5, pp. 507–514, 2018.

[8] H. Mortazavi., H. Mehrjerdi., M. Saad, S. Lefebvre, and D. Asber. "A Monitoring Technique for Reversed Power Flow Detection with High PV Penetration Level", *IEEE Transactions on Smart Grid*, vol. 6, no.5, pp. 2221-2232, Sep 2015.

[9] H Mehrjerdi, "Off-grid solar powered charging station for electric and hydrogen vehicles including fuel cell and hydrogen storage", *International journal of hydrogen Energy*, vol. 44, no. 23, pp. 11574-11583, 2019.

[10] F. Ha and A. Abdennour, "Optimal use of kinetic energy for the inertial support from variable speed wind turbines," *Renew. Energy*, Vol. 80, pp. 629–643, 2015.

[11] Hasan Mehrjerdi, Elyas Rakhshani, "Correlation of multiple time-scale and uncertainty modelling for renewable energy-load profiles in wind powered system," *Journal of Cleaner Production*, Elsevier, Vol. 236, 2019.

[12] F. M. Gonzalez-Longatt, "Effects of the synthetic inertia from wind power on the total system inertia: Simulation study," in Proc. *2nd Int. Symp. Environ. Friendly Energies Appl.*, 2012, pp. 389–395.

[13] J. Driesen and K. Visscher, "Virtual synchronous generators," in Proc. *IEEE Power & Energy Soc. General Meeting*, 2008, pp. 1–3.

[14] M. C. Luis and A. Enrique, "On the provision of frequency regulation in low inertia AC grids using HVDC systems," *IEEE Trans. Smart Grid*, Vol. 7, Issue 6, 2016..

[15] M. Guan, W. Pan, J. Zhang, Q. Hao, J. Cheng, and X. Zheng, "Synchronous generator emulation control strategy for voltage source converter (VSC) stations," *IEEE Trans. Power Syst.*, Vol. 30, No. 6, pp. 3093–3101, Nov. 2015.

[16] J. Alipoor, Y. Miura, and T. Ise, "Power system stabilization using virtual synchronous generator with alternating moment of inertia," *IEEE J. Emerg. Sel. Topics Power Electron.*, Vol. 3, No. 2, pp. 451–458, Jun. 2015.

[17] E. Rakhshani, J. Rueda Torres, Mart van der Meijden, and P. Palensky, "Determination of Maximum Wind Power Penetration Considering Wind Turbine Fast Frequency Response", 2019 *IEEE PowerTech conference*, Milan, 2019, pp. 1-6.

[18] E. Rakhshani, D. Remon, A. Mir Cantarellas, and P. Rodriguez, "Analysis of derivative control based virtual inertia in multi-area high-voltage direct current interconnected power systems," *IET Gener. Transm. Distrib.*, Vol. 10, No. 6, pp. 1458–1469, 2016.

[19] J. Zhu and J. M. Guerrero, "Generic inertia emulation controller for multiterminal voltage-source-converter high voltage direct current systems," *IET Renew. Power Gener.*, Vol. 8, No. 7, pp. 740–748, 2014.

[20] E. Rakhshani, D. Gusain, V. Sewdien, Jose Luis Rueda Torres, Mart Van der Meijden, "A Key Performance Indicator to Assess the Frequency Stability of Converter Dominated Power System", *IEEE Access*, vol. 7, pp. 130957-130969, 2019.

[21] E. Rakhshani, D. Remon, A. M. Cantarellas, J. M. Garcia and P. Rodriguez, "Virtual Synchronous Power Strategy for Multiple HVDC Interconnections of Multi-Area AGC Power Systems," *IEEE Transactions on Power Systems*, Vol. 32, No. 3, pp. 1665-1677, May 2017.

[22] A. Khaki Sedigh, "*Modern Control Systems*", Iran, University of Tehran Press, 2003.

[23] K.Ogata, "*Modern Control Engineering*", Prentice – Hall, 1990.

[24] B. Friedland, "*Control System Design : An Introduction to State – Space Methods*", McGraw - Hill, 2003.

[25] I. Mohammad Hosseini Naveh and J.Sadeh, "Appication of Modern Optimal Control in Power System: Damping Detrimental Sub-Synchronous Oscillations", Published in *MATLAB for Engineers – Applications in Control, Electrical Engineering, IT and Robotics*, Chapter Book, InTech Press, 2011.

[26] E. Rakhshani and J.Sadeh, "A reduced-order estimator with prescribed degree of stability for two-area LFC system in a deregulated environment", Published in *IEEE Power Systems (PES) Conference and Exposition*, 2009.